Investigation of the electrostatic properties of humic substances by fluorescence quenching

ARTICLE *in* ENVIRONMENTAL SCIENCE AND TECHNOLOGY · FEBRUARY 1992

Impact Factor: 5.33 · DOI: 10.1021/es00026a008

3 AUTHORS, INCLUDING:

Sarah Green
Michigan Technological University
56 PUBLICATIONS **2,345** CITATIONS

SEE PROFILE

(19) Wershaw, R. L.; Pinckney, D. J. *J. Res. U.S. Geol. Surv.* **1973**, *1*, 701-707.
(20) Verwey, E. J. W.; Overbeek, J. Th. G. *Theory of the Stability of Lyophobic Colloids*; Elsevier: Amsterdam, 1948.
(21) Dzombak, D. A.; Morel, F. M. M. *Surface Complexation Modeling: Hydrous Ferric Oxide*; Wiley: New York, 1990.
(22) Manning, G. S. *Acc. Chem. Res.* **1979**, *12*, 443-449.
(23) Zimm, B. H.; LeBret, M. *J. Biomol. Struct. Dyn.* **1983**, *1*, 461-471.
(24) Kotin, L.; Nagasawa, M. *J. Chem. Phys.* **1962**, *36*, 873-879.
(25) Delville, A. *Chem. Phys. Lett.* **1980**, *69*, 386-388.
(26) Mandel, M. In *Encyclopedia of Polymer Science and Engineering*; Mark, H. F., Bikales, N. M., Overberger, C. G.; Menges, G., Eds.; Wiley: New York, 1988; Vol. 11, pp 739-829.
(27) Bartschat, B. M. M.S. Thesis, Massachusetts Institute of Technology, Cambridge, MA, 1990.
(28) Müller, H. *Kolloidchem. Beih.* **1928**, *26*, 257-310.
(29) Wall, F. T.; Berkowitz, J. *J. Chem. Phys.* **1957**, *26*, 114-122.
(30) Bowles, E. C.; Antweiler, R. C.; MacCarthey, P. In *Humic Substances in the Suwannee River, Georgia: Interactions, Properties, and Proposed Structures*; Averett, R. C., Leenheer, J. A., McKnight, D. M., Thorn, K. A. Eds. *Open-File Rep.—U.S. Geol. Surv.* **1989**, *No. 87-557*, 205-229.
(31) Cabaniss, S. E. Ph.D. Thesis, University of North Carolina, Chapel Hill, 1986.
(32) Westall, J. C. MICROQL II. Computation of Adsorption Equilibria in BASIC. Technical Report, Swiss Federal Institute of Technology, EAWAG: Dübendorf, Switzerland, 1979.
(33) Morel, F. M. M. *Principles of Aquatic Chemistry*; Wiley: New York, 1983.
(34) Noyes, T. I.; Leenheer, J. A. In *Humic Substances in the Suwannee River, Georgia: Interactions, Properties, and Proposed Structures*; Averett, R. C., Leenheer, J. A., McKnight, D. M., Thorn, K. A., Eds. *Open-File Rep.—U.S. Geol. Surv.* **1989**, *No. 87-557*, 231-250.
(35) Susetyo, W.; Dobbs, J. C.; Carreira, L. A.; Azarraga, L. V.; Grimm, D. M. *Anal. Chem.* **1990**, *62*, 1215-1221.
(36) Hering, J. G.; Morel, F. M. M. *Environ. Sci. Technol.* **1988**, *22*, 1234-1237.
(37) Martell, A. E.; Smith, R. M. *Critical Stability Constants*; Plenum: New York, 1977; Vol. III, pp 200-201.
(38) Kielland, J. *J. Am. Chem. Soc.* **1937**, *59*, 1675-1678.

Received for review February 25, 1991. Revised manuscript received October 14, 1991. Accepted October 23, 1991. This work was supported in part by Grants R817371-01-0 from EPA and OCE-9116427 from NSF.

Investigation of the Electrostatic Properties of Humic Substances by Fluorescence Quenching

Sarah A. Green,*,† François M. M. Morel,*,‡ and Neil V. Blough*,§

Department of Chemistry, Woods Hole Oceanographic Institution, Woods Hole, Massachusetts 02543, and Ralph M. Parsons Laboratory, Department of Civil Engineering, Massachusetts Institute of Technology, Cambridge, Massachusetts 02139

■ A fluorescence quenching technique was employed to explore the electrostatic properties of fulvic acid (FA) and humic acid (HA). Cationic nitroxides were found to be up to 16 times more effective than neutral analogues in quenching the fluorescence of humic materials. This result is attributed to the enhanced Coulombic attraction of cations to the anionic FA or HA surface and is interpreted as an estimate of surface potential. Reduction of molecular charge at low pH and shielding of charge at high ionic strength produced diminished enhancements, consistent with this interpretation. High molecular weight fractions of HA have a higher apparent surface potential than lower molecular weight fractions, indicating that larger humic molecules may have an enhanced ability to bind metal ions.

Introduction

Humic substances play an important role in controlling trace-metal speciation in natural waters. As the prevalent chromophores in most aquatic environments, they are also responsible for initiating numerous photochemical transformations of both organic compounds (*1*, *2*) and trace metals (*3*). With the goal of better understanding these processes, a great deal of effort has gone toward modeling the interactions between metal ions and humic materials (*4*, *5*). Recently the electrolyte character of fulvic acids and humic acids has been considered in terms of its impacts on both cation binding (*6*, *7*) and rates of photochemical reactions (*8*).

A current approach to modeling metal binding by humic acids over variable pH and ionic strength regimes explicitly includes a Coulombic term in addition to intrinsic binding constants (*6*, *7*, *9*, *10*). In these models, intrinsic binding constants remain invariant with pH and ionic strength while the Coulombic term is allowed to vary as predicted by electrostatic theory. Initial application of this type of model has been successful in this laboratory (*6*) in fitting copper titration data without relying on such physically unsatisfying concepts as binding constants that vary with ionic strength.

Natural humic substances are oligoelectrolytes which are predicted to have a large negative surface potential, primarily due to deprotonated carboxylic acid groups. This negative potential is expected to result in increased cation concentrations near the humic surface. Experimentally this has been confirmed indirectly by Blough (*8*), who has shown that radicals produced by irradiation of humic acid are more efficiently scavenged by a cationic species than by analogous neutral or anionic compounds. Thus, electrostatic effects can influence the competition between charged and neutral species (e.g., oxygen) for photoproduced radicals. Similarly, this region of enhanced cation concentration around humic molecules may be an important zone for thermal and photoinduced metal reduction/oxidation, since an ion here may be sufficiently close to act as an electron acceptor/donor, yet be able to diffuse away before undergoing back electron transfer.

In this work our goal is to provide an experimental basis for models that require information about the electrostatic characteristics of humic materials. We have employed a fluorescence quenching technique to explicitly examine the local excess of cations around fulvic acid molecules and

† MIT-WHOI Joint Program in Oceanography.
‡ Massachusetts Institute of Technology.
§ Woods Hole Oceanographic Institution.

 0013-936X/92/0926-0294$03.00/0

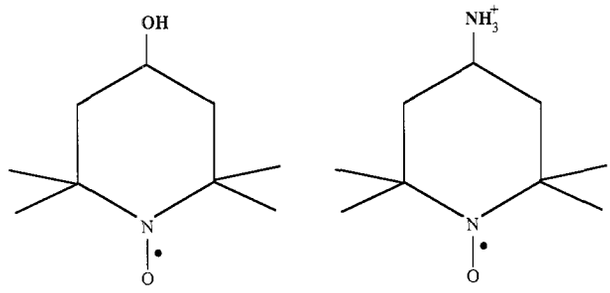

a b

Figure 1. Quenchers employed in this study: (a) 4-hydroxy-tempo (tempol) and (b) 4-amino-tempo (tempamine).

to place limits on the effective fulvic acid surface potential as a function of pH and ionic strength. Also, the relative surface potentials of different size classes of the humic molecules are compared. Suwannee River fulvic acid (FA) and Suwannee River humic acid (HA) were selected as representitive humic substances.

Experimental Rationale

Among species known to be effective quenchers of fluorescence, paramagnetic compounds such as Cu^{2+}, O_2, and stable nitroxide radicals are particularly useful. Static quenching, produced by direct coordination of Cu^{2+}, Fe^{3+}, and other metal ions, has been employed in previous studies of cation binding to humic substances (*11–14*). Unlike these metals, nitroxides do not coordinate to these materials and may therefore be employed as dynamic quenchers to investigate weaker nonbonding interactions. Stable nitroxide radicals are, like oxygen, effective quenchers of excited singlet states (*15*), but have the advantage of a higher aqueous solubility. In addition, they are available in a variety of charged forms, making them especially well suited to studies of electrostatic effects. In these experiments we employ principally the neutral 4-hydroxy-tempo (tempol), the cationic 4-amino-tempo (tempamine) (Figure 1) and, to a lesser extent, the anionic 3-carboxy-proxyl and the cationic quaternary amine 4-(trimethylamino)-tempo to probe the anionic character of humic substances.

To interpret the data, we employ a simple physical model developed within the framework of the standard Stern–Volmer analysis (*16*):

$$F \xrightarrow{h\nu} F^* \tag{1}$$

$$F^* \xrightarrow{k_r} F + h\nu \tag{2}$$

$$F^* \xrightarrow{k_{nr}} F \tag{3}$$

$$F^* + Q \underset{k_{-dif}}{\overset{k_{dif}}{\rightleftharpoons}} [F^*Q] \xrightarrow{k_{quen}} F + Q \tag{4}$$

In the presence of quencher, Q, the excited fluorophore, F*, can undergo three fates: (1) radiative relaxation to the ground state (F) with emission of a photon (eq 2), (2) nonradiative relaxation to the ground state (eq 3), or (3) a diffusional encounter to form a collision complex that provides a rapid, nonradiative relaxation pathway to the ground state (eq 4). Under constant illumination, the ratio of the fluorescence intensities in the absence (F_0) and presence (F) of quencher is given by the Stern–Volmer equation

$$F_0/F = 1 + k_q\tau[Q] \tag{5}$$

where

$$k_q = k_{quen}k_{dif}/(k_{quen} + k_{-dif}) \tag{6}$$

and

$$\tau = 1/(k_r + k_{nr}) \tag{7}$$

is the excited state lifetime of the unquenched fluorophore. If $k_{quen} \gg k_{-dif}$, then $k_q = k_{dif}$ and the quenching becomes diffusion controlled. Because nitroxides quench excited singlet states at or near the diffusion-controlled limit (*17*), we consider k_{quen} to be large with respect to k_{-dif} throughout this discussion.

In practice, the ratio, F_0/F, is determined at a series of quencher concentrations and the slope, equal to $k_q\tau$, is determined from the plot of F_0/F vs [Q]. As we show below, this slope is substantially larger for the cationic, as compared to the neutral, quenchers. Because $k_q \approx k_{dif}$ this increased slope cannot result from a change in the efficiency of quenching within the collision complex (k_{quen} or k_{-dif}, eq 6). Instead, this result indicates that the cationic quencher is not homogeneously distributed in solution, but rather is attracted by Coulombic forces to the vicinity of the anionic FA. In the kinetic analysis, the increased slope obtained for the cationic quenchers is attributed to an enhanced diffusion-controlled rate constant (vide infra). A simpler, though less precise, interpretation is the pseudostatic model in which the increase is ascribed to an excess concentration of quenchers at the FA surface. In either case, the observed effects may be quantified by defining the term λ_{meas} as the measured electrostatic enhancement factor, such that

$$[Q]_L = \lambda_{meas}[Q]_B \tag{8}$$

where $[Q]_B$ is the bulk quencher concentration, $[Q]_L$ is the apparent "local" quencher concentration around the fluorophore, and λ_{meas} is defined to be unity for neutral quenchers. Thus, $[Q]_L$ is the concentration of neutral quenchers which would be required to obtain the same degree of quenching as is measured for a concentration of cationic quenchers equal to $[Q]_B$. Equation 5 can then be reformulated as

$$F_0/F = 1 + k_q\tau\lambda_{meas}[Q] \tag{9}$$

A Stern–Volmer plot for the neutral quencher has a slope of $K_N = k_q\tau$, while for a cationic quencher the slope is $K_C = K_N\lambda_{meas}$; the ratio of slopes from the two plots gives λ_{meas}. In this study, we use λ_{meas} to make relative comparisons among several samples and then invoke the more detailed analyses, described below, to study the ionic strength dependence of λ_{meas} for FA.

Pseudostatic Analysis. The interpretation of the parameter λ_{meas} is not necessarily straightforward, although it is clearly related to the electrostatic characteristics of the fluorophore. In its simplest interpretation (*18*), the local quencher concentration in the vicinity of the fluorophore is related to $[Q]_B$ through the Boltzmann equation

$$[Q]_L = [Q]_B \exp(-\Psi'/k_BT) \tag{10}$$

which gives

$$\lambda_{meas} = \exp(-\Psi'/k_BT) \tag{11}$$

where Ψ' is the apparent attractive electrostatic potential, k_B is the Boltzmann constant, and T is the absolute temperature. This is equivalent to defining a sphere around F, in which all possible quenchers are contained and are subject to an average potential, Ψ'. This simple approach has the advantage of being intuitively accessible, but it is important to acknowledge that it is a rough approximation because it neglects the dynamic nature of the quenching and the distance dependence of Ψ.

Diffusional quenching is accomplished not only by quenchers immediately adjacent to an excited fluorophore, but also by those that can reach one during its excited-state lifetime. Since Ψ decreases as a function of distance, $[Q]_L$ also decreases radially from the surface. Thus, neither Ψ' nor $[Q]_L$ in eq 10 are well-defined entities, but they actually represent distance-weighted averages along the gradient from the surface to some distance away. This effect is moderated somewhat by geometric considerations since the probability that a quencher will diffuse to a fluorophore decreases very rapidly with their separation distance. The overall result is that λ_{meas} does not directly represent the potential at the surface, as is suggested by eq 11, but is smaller than that limiting value due to participation by more distant quenchers (subject to a lower potential).

$\Psi(r)$ is a function of the size and charge of the macromolecule, and of the ionic strength, I (M), through the Debye length, $\kappa = 0.327\sqrt{I}$ (Å^{-1}). For small, spherically symmetrical potentials, the Debye–Hückel equation gives (*19*)

$$\frac{\Psi(r)}{k_B T} = z r_0 \frac{\exp[\kappa(R - r)]}{r(1 + \kappa R)} \tag{12}$$

where z is the product of charges on the macromolecule and quencher, R is the radius of closest approach of counterions to the macromolecule, and r is the distance from the center of the macromolecule; r_0 (Onsager length) is equal to 7.1 Å in water at 25 °C. For large Ψ, eq 12 is not valid and numerical calculations must be employed (*6*).

Kinetic Analysis. A simple kinetic analysis (*20*) includes the dynamics of the problem, and in cases where the Debye–Hückel equation is applicable, an analytical expression for the steady-state quenching rate is obtained. In this approach the Stern–Volmer constant, k_q (eq 5), is given by

$$k_q = 4\pi D\beta \tag{13}$$

where

$$\beta^{-1} = \int_R^\infty \frac{\exp(\Psi(r)/k_B T)}{r^2}\, dr \tag{14}$$

and D is the sum of diffusion coefficients for Q and F, and R is the sum of their radii. For $\Psi = 0$ (e.g., neutral quencher), $\beta = R$. With $\Psi(r)$ defined by eq 12, an attractive potential results in

$$\beta = -z r_0 \exp(z r_0 \kappa') \tag{15}$$

with

$$\kappa' = \kappa/(1 + R\kappa) \tag{16}$$

Then we have

$$\lambda = \beta/R = \frac{-z r_0}{R} \exp(z r_0 \kappa') \tag{17}$$

This predicts that a plot of ln λ vs κ' will be linear with slope $z r_0$. κ' is a function of molecular radius (eq 16), so R remains an adjustable parameter.

The static definition of λ, described by eq 11, and the kinetically derived expression (eq 17) represent two limiting cases. The first case, in which dynamics are ignored, is equivalent to assuming that the product $D\tau$ is small, so that only quenchers that are very close to a fluorophore can reach it before it emits a photon. The second case relies on the assumption of a steady-state distribution of quenchers around each excited fluorophore, which is only obtained for large values of $D\tau$. The pseudostatic model predicts fairly large values for λ because it only accounts for the participation of those quenchers most strongly affected by the attractive potential. The dynamic model predicts quite small values for λ because at long times, when a steady state has been achieved, the probability that an excited fluorophore will still have a quencher in close proximity is small and the rate of quenching is therefore governed by more distant quenchers (see Appendix). At intermediate times, applicable to most fluorophores, we expect λ_{meas} to fall somewhere between these two extremes, and so we do not expect either model to exactly describe the quenching data. We take two approaches to modeling fulvic acid quenching as a function of ionic strength. First, we apply the pseudostatic model, but account for distance averaging by choosing Ψ' (eq 11) equal to the potential at a distance, r' (instead of at the surface), where Ψ' is given by eq 12 and r' is treated as a fitting parameter. In the second model, we graph ln λ vs κ' according to eq 17 and discuss our results in this context.

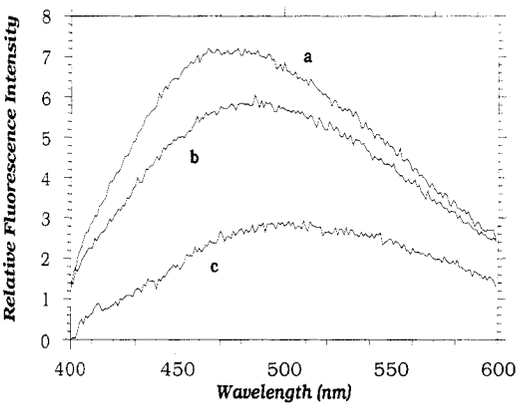

Figure 2. Fluorescence spectra of HA fraction C, in 10 mM borate buffer: (a) no quencher added, (b) with 8.2 mM tempol, and (c) with 8.2 mM tempamine. Spectra have been corrected for dilution, but not for inner filter effect, which leads to an apparent red shift in peak maxima (b and c) due to light absorption by the nitroxides in the range 400–460 nm.

Fluorescence of Humic and Fulvic Acids. Absorption of light by humic substances decreases approximately exponentially throughout the ultraviolet and visible wavelength regime (*21*). Light absorption in the range 300–400 nm results in fluorescence emission having a broad maximum near 460 nm (Figure 2); with longer wavelength excitation the emission peak decreases in intensity and shifts to the red. For Suwannee River fulvic acid, the overall fluorescence maximum occurs with excitation at 350 nm and emission at 460 nm. This is also the case for bulk Suwannee River humic acid, although individual size fractions of this material show slightly different fluorescence characteristics (vide infra). Broad, overlapping excitation and emission spectra and shifts in emission maxima with excitation wavelength are indicative of multiple fluorophores in these materials. This is confirmed through the measurement of complex, multiexponential fluorescence decay kinetics which suggest a minimum of three fluorescing species with lifetimes ranging from <1 to 6 ns (*22*).

In principle, the Stern–Volmer equation strictly applies only to species exhibiting a monoexponential fluorescence decay, a possible complication in the quenching of humic samples. In practice, however, significant nonlinearity in these plots would be detectable only if fluorescence lifetimes of the several species present differed by over 1 order of magnitude and at very high quencher concentrations (>50 mM); neither condition applies in this study. (It follows that a linear Stern–Volmer plot does not necessarily indicate the presence of a single, unique fluorophore.) The

measured lifetimes of humic and fulvic acid fluorophores are in the range of <1 to ~7 ns (*22–25*); fewer than 5% of the fluorophores present have lifetimes longer than 2.5 ns (*22, 25*). In eq 1, τ becomes a weighted average of the true lifetimes. Because we do not rely on τ explicitly, only its constancy, its actual value is of secondary importance to this discussion.

A detailed theory of fluorescence quenching, incorporating time dependence and multiple lifetimes, has been derived by Szabo (*26*). However, for our purposes it makes little sense to apply such in-depth theories to a system that includes ill-defined values of τ, diffusion coefficients, and R. Indeed, if we are to retain generality for natural samples, it is reasonable to neglect differences in detail among individual molecules and to focus on what can be learned from these heterogeneous samples. In this spirit we shall first compare λ_{meas} values for FA and several size fractions of HA, at a fixed ionic strength of 5 mM (10 mM borate buffer). Then for FA we measure λ_{meas} as a function of ionic strength and make comparisons with a model compound, perylenetetracarboxylic acid. We then examine our measured values in the context of the pseudostatic (eq 11) and kinetic (eq 17) models using some reasonable assumptions about the average size and charge on humic molecules.

Experimental Section

General Procedures. Standard Suwannee River fulvic acid and humic acid were obtained from the International Humic Substance Society (IHSS). Fulvic acid was used as received; humic acid was acid washed to remove labile metals, as recommended by Hering (*27*), with the exclusion of the drying step. Perylenetetracarboxylic acid (PTC) was obtained from Aldrich as the dianhydride and was hydrolyzed in 25 mM NaOH. An NMR spectrum of PTC in D_2O/NaOD did not reveal any impurities or (partial) anhydride in solution. Water was from a Millipore Milli-Q system. 4-Hydroxy-tempo (tempol) and 4-amino-tempo (tempamine) were obtained from Aldrich; 4-(trimethylamino)-tempo(I^-) (trimethyl-tempamine) and 3-carboxy-proxyl were purchased from Sigma or Molecular Probes. Trimethyl-tempamine was passed through an anion-exchange column to replace I^- with Cl^-; the other compounds were used as received. Concentrated stocks (0.2–0.4 M) of these were made in water and their precise concentrations determined by absorption at 434 nm (ϵ = 12.6 M^{-1} cm^{-1}). In the experiments using tempamine and 3-carboxy-proxyl, the pH of stock solutions was adjusted to match that of the fulvic or humic sample being titrated.

Absorbance spectra were measured on an HP 8451A diode array spectrophotometer with 2-nm resolution. Fluorescence data were collected on an SLM Aminco SPF-500C fluorometer in ratio mode; the excitation and emission bandpasses were typically 4 and 5 nm, respectively. A 1-cm quartz cell was used for all optical measurements. Reported emission spectra have been corrected for instrument response with the software provided by the company.

Size Fractionation. HA was separated into 10 size fractions by gel chromatography using Sephadex G-50 (Sigma) eluted with 10 mM borate buffer (pH = 9.1). HA was not retained on either Sephadex G-10 or G-25 columns, indicating that chemical interactions with the gel do not occur in this buffer system. The column was 21.5 cm in length, with internal diameter 1.5 cm; flow rate was 0.56 mL/min. A sample of HA was preequilibrated in the eluting buffer and 0.5 mL of solution was applied to the column. Nine fractions of 0.9 mL each, and a tenth of 5.9 mL, were collected. Five samples, A–E, were chosen for quenching experiments, where A corresponds to fraction 2, B to 4, C to 6, D to 8, and E to 10. Fractions (except E) were diluted in buffer to an OD at 350 nm of 0.072, 0.063, 0.030, 0.013, and 0.013 for A–E, respectively.

Quenching. Concentrated stock solutions (~0.5 g/L) of FA were prepared in water, filtered (0.2 μm), and kept refrigerated in the dark. No difference in absorbance, fluorescence, or quenching properties was observed between fresh and stored samples. Solutions for quenching experiments were made by dilution of stocks into 10 mM acetate or borate buffers, providing an initial ionic strength of 5 mM. Ionic strength was increased, when required, by addition of the appropriate volumes of 0.4 or 4.0 M NaCl. The contribution of probe nitroxides is not included in the reported ionic strengths. Fulvic acid concentrations were approximately 5 mg/L; absorbance at 350 nm was 0.03 ± 0.005 (1-cm cell).

In quenching experiments, 2-mL solutions of fulvic or humic acids, or PTC, were titrated with 5–10-μL increments of nitroxide stock solutions to a final quencher concentration of ~10 mM. Fluorescence emission of FA was monitored at 460 nm with excitation at either 350 or 365 nm. HA fractions were excited at 350 nm with emission measured at 520 (A), 500 (B), 475 (C), or 465 nm (D and E). Excitation and emission wavelengths for PTC were 468 and 511 nm, respectively. Samples were illuminated only during actual measurement to avoid possible photobleaching or other photoinduced reactions. No change in fluorescence was observed when solutions were deoxygenated through bubbling with N_2, so no further attempt was made to exclude oxygen. The pH did not change by more than 0.1 pH unit during any titration.

Fluorescence data were corrected for dilution, weakly fluorescent impurities in the nitroxide stocks, and inner filter effect (*28*). Inner filter corrections did not exceed 25% for the highest nitroxide concentration employed and were nearly equivalent for both tempol and tempamine due to their almost identical absorption spectra. Data were graphed according to the Stern–Volmer equation (eq 5). Plots were linear with an intercept of 1.00 ± 0.02, except in a few cases where a decrease in slope was observed at high quencher concentrations. These deviations were observed primarily during titrations with trimethyl-tempamine and may be due to steric effects associated with the bulk of the three methyl groups surrounding the positive charge on this quencher. Initial slopes for trimethyl-tempamine were the same as those for tempamine, indicating that the primary amine in the latter compound is not contributing to the observed quenching. Tempamine was employed for subsequent experiments.

In a second set of experiments, solutions containing fulvic acid, either alone, with tempol (~4 mM), or with tempamine (~4 or 7 mM), were titrated in parallel with 0.4 or 4.0 M NaCl. The salt titration in the absence of nitroxide was used to correct for (small) changes in fulvic acid fluorescence due to ionic strength alone; other corrections were as noted above. From these data, λ was calculated for each addition from the rearranged Stern–Volmer equation:

$$\lambda = [(F_0/F) - 1]/K_N[Q]_B$$

where K_N is obtained from quenching by tempol (λ = 1).

Results and Discussion

Suwannee River fulvic and humic acid fluorescence was effectively quenched by the neutral and cationic nitroxides employed in this study (Figure 2). Emission appeared to be uniformly suppressed from 370 to 650 nm (excitation at 350 nm) although light absorption by the nitroxide itself

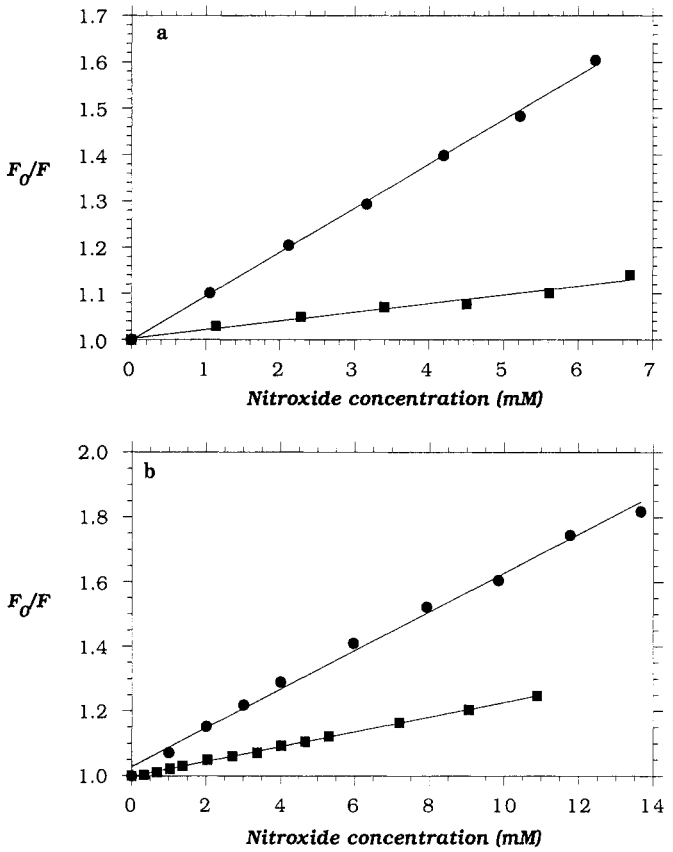

Figure 3. Stern–Volmer plots of quenching of fulvic acid fluorescence by tempol (squares) or tempamine (circles): (a) pH = 8.8, I = 5 mM; (b) pH = 4.6, I = 12 mM.

(peak maximum at 435 nm) makes this difficult to ascertain. No new emission or absorption bands, which would indicate specific excited- or ground-state interactions between humics and nitroxides, were observed.

Suwannee River Fulvic Acid. FA solutions were titrated with tempol under a variety of pH and ionic strength conditions. Stern–Volmer plots (Figure 3) were linear and reproducible to within 4%. No systematic change in the slope (K_N) was observed over the pH and ionic strength range studied (pH = 4–9, I = 5–300 mM), indicating that the local concentration of neutral quencher is not significantly influenced by these factors. A value of K_N = 18.6 M^{-1}, an average of 50 determinations (including both slopes from Stern–Volmer plots and single-point measurements from NaCl titrations), represents the baseline, dynamic quenching coefficient and was used as a point of comparison for the charged quenchers. Quenching of FA fluorescence by cationic nitroxides, tempamine and trimethyl-tempamine at pH = 9.1 and I = 5 mM, resulted in linear Stern–Volmer plots with slopes 5.1-fold greater than those obtained for tempol (Table I). A smaller increase (3.5-fold) was measured at pH = 4.6. The anionic nitroxide, 3-carboxy-proxyl, was an ineffective quencher, giving Stern–Volmer plots with a slope of 0 within experimental uncertainty. Since in each case the identical nitroxide moiety is responsible for quenching, there should be no intrinsic differences in quenching efficiency among these compounds. All observed variations are therefore attributed to Coulombic interactions.

Suwannee River Humic Acid. HA, which is more polydisperse than the FA (*29*, *30*), was used to examine changes in surface potential with molecular size. An empirical size separation was accomplished by gel permeation chromatography. Because gel filtration does not provide accurate molecular weight values for humic substances

Table I. Fluorescence Peak Maxima and Relative Efficiencies, Measured Stern–Volmer Quenching Constants K_N (Tempol) and K_C (Tempamine), and Ratios (λ_{meas}) for FA and HA Fractions and PTC

sample	fluor max, nm	F_0/abs[a]	K_N, M^{-1}	K_C, M^{-1}	λ_{meas}
FA					
pH = 9.1	460	11.7	18.6	94.9	5.1
pH = 4.6	460	11.6	18.6	65.1	3.5
HA fractns[b]					
A	530	0.49	9.5	160.4	16.9
B	510	0.99	15.4	159.1	10.3
C	477	2.5	14.0	136.4	9.7
D	467	4.5	10.8	84.9	7.9
E	470	5.7	20.5	61.2	3.0
perylenetetra-carboxylic acid	511		32.2	122.3	3.8

[a] Fluorescence at peak maximum divided by absorbance at 350 nm, background subtracted. [b] HA fraction A contains the largest molecular weight molecules, E the smallest.

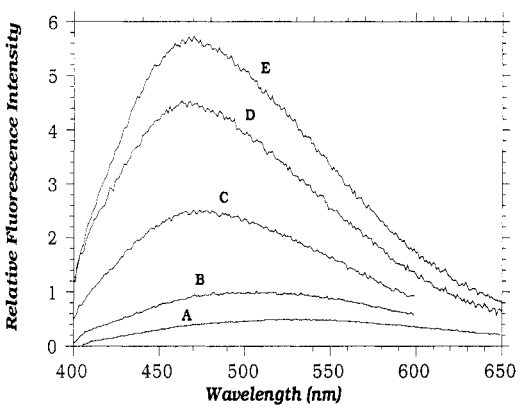

Figure 4. Fluorescence emission scans of HA size fractions A–E. Intensity has been normalized to absorbance at the exciting wavelength (350 nm); excitation and emission bandpasses were 5 nm.

when calibrated against globular proteins (*30–32*), we refrain from estimating precise molecular weights of our fractions. This technique does, however, give a qualitative separation by size (*31*, *32*). Molecular weight ranges estimated by analytical ultracentrifugation (*30*) are 2000–10 000 for HA and 1000–2000 for FA from this source. Other workers report somewhat lower molecular weight values for FA: 860 by flow field-flow fractionation (*29*), and 740 by vapor-pressure osmometry (*33*).

For all fractions, fluorescence efficiency (F_0/absorbance) decreased with increasing size (Figure 4, Table I), a trend which has been previously observed (*34*, *35*). In addition, emission spectra for the large-sized HA fractions were red-shifted relative to FA emission. Some variation in K_N was observed among the humic samples, which, along with the shifts in emission wavelength, could indicate the dominance of different fluorophores or different fluorophore microenvironments in each fraction. To a first approximation, differences in fluorescence yield or energy do not affect determinations of λ_{meas} because quenching by neutral and cationic nitroxides is compared for each sample. This *can* pose a problem when fluorescence is extremely low because quenching by the neutral nitroxide, tempol, becomes difficult to measure accurately. For this reason, more concentrated solutions (higher absorbance) were employed for quenching experiments with fractions A and B.

Quenching by the cationic nitroxide increased significantly with molecular size (Table I). Fraction A, containing the highest molecular weight species, exhibited

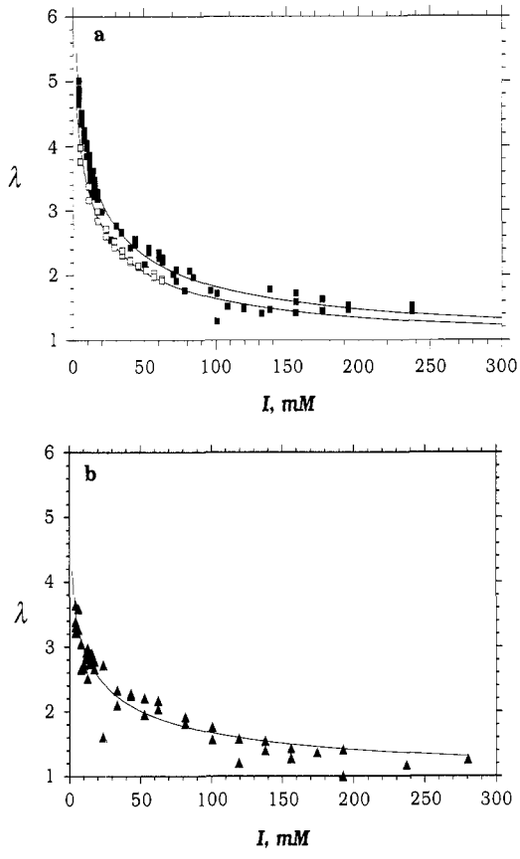

Figure 5. λ vs ionic strength for FA (■) and PTC (□) at pH = 9.1 (a) and pH = 4.6 (b). The lines are plots of the Debye–Hückel potential at 5 Å from the surface, for R = 8 Å, and z = −4.3 (a) or z = −3.0 (b).

both the highest degree of quenching by tempamine and the lowest by tempol, giving it the largest λ_{meas} of any sample in this study. Fraction E, containing the lowest molecular weight species, showed the lowest λ_{meas} in this group. If molecular charge increases proportionally to volume, then the potential at the surface, $\Psi(R)$, increases as $R^2/(1 + \kappa R)$ (eq 12, with $z \propto R^3$, $r = R$). Our data show a strong correlation between λ_{meas} and R, consistent with this prediction.

Data suggest that acid content per carbon, specific volume, and therefore charge per volume do not differ greatly between humic and fulvic acids. Total (carboxyl and phenolic) acidity per gram (*36*) is nearly identical for FA (7.6 mmol/g) and HA (7.8 mmol/g), and their molar volumes (*30*) (0.46 and 0.51 cm^3/g, respectively) are within 10% of each other. However, carboxyl groups are relatively more important in FA (6.1 mequiv/g) than in HA (4.9 mequiv/g) (*36*). Thus, at pH = 9.1, HA should have a smaller overall charge per gram than FA; their higher molecular weights give HA a larger charge per *molecule* than FA. These data represent whole HA; there are no independent data available on possible variation of these parameters among size fractions.

Ionic Strength Effects. FA solutions were titrated with NaCl to examine the effect of ionic strength on quenching by cationic quenchers. At pH = 9.1, λ_{meas} decreased rapidly in the range of 5–50 mM NaCl, with more gradual decreases at higher salt concentrations (Figure 5). The trend is the same at pH = 4.6, but the magnitude of λ_{meas} is lower throughout this ionic strength range. Thus, sodium ions can effectively shield the electrostatic interactions between the cationic nitroxide and the fulvic acid and thus decrease the apparent surface potential of fulvic acid molecules.

Overall, these data fit our expectations for the behavior of oligoanionic macromolecules. At high pH all carboxyl (and perhaps some of the phenolic) groups are dissociated and the molecular charge is large, while at pH 4.6 some of these groups are protonated and the total charge is lower. The lack of complete charge neutralization at this pH is consistent with the carboxylic acid (pK_a < 3–5) content of these materials. In addition, the HA data confirm the expectation that large humic molecules have a greater surface potential than small ones.

These dramatic changes in λ_{meas} lend support to models that incorporate electrostatic terms to account for variations in acidity or metal binding constants with ionic strength. Electrostatic terms should be of particular importance in transition zones, such as estuaries, where I increases from <5 mM to 0.7 M as river water and seawater mix. Size distributions in humic substances may also influence the transport and ultimate fates of some metal species which may be preferentially bound to the larger organic molecules.

Model Compound: Perylenetetracarboxylic Acid. PTC was employed as a model compound because its charge (−4) and size (R = 6.5 Å) are comparable to those estimated for FA. Quenching of PTC by tempol gave a K_N approximately 2-fold larger (32.2 M^{-1}) than that measured for FA (18.6 M^{-1}). This result is expected (eq 5) based on the longer fluorescence lifetime of PTC (~5.4 ns) as compared with FA. The Stern–Volmer plot obtained from quenching by tempamine showed upward curvature; this is predicted when the degree of quenching is high and the steady-state limit is not reached (*28*, *37*). Higher order corrections to the Stern–Volmer equation predict nonlinearity, but the curvature is slight so we may safely neglect this correction. We therefore concentrate on the linear portion of the plot, which leads to $K_N\lambda$ = 122.3 M^{-1}. The ionic strength dependence of quenching by tempamine was remarkably similar to that of FA (Figure 5), with λ_{meas} values for PTC falling slightly lower for ionic strengths of 5–60 mM.

Pseudostatic and Kinetic Model Fits

The qualitatively reasonable behavior of our results encouraged an attempt to extract more quantitative information about FA from these data, using the pseudostatic and kinetic analyses presented under Experimental Rationale.

Although it ignores important aspects of the quenching process, we observe that the pseudostatic model (eq 11) accurately reproduces the shape of the plots of λ vs ionic strength, with Ψ' taken as the Debye–Hückel potential at a distance (r') of 11 Å from the center of the FA molecule (Figure 5). For this fit we chose z = −4.3 and R = 8 Å, in accordance with Aiken et al. (*33*). PTC data can be fit with z = −4, R = 6.5, and r' = 15 Å.

While the kinetic model is not expected to accurately predict absolute quenching rates, the relative change in rate with ionic strength may still be examined. Because κ' must be calculated from R, which is not well constrained, determination of z from eq 17 is not unambiguous. Thus, the model compound, PTC, was used to aid in choosing the appropriate range of values for R. Figure 6a shows plots of ln λ vs κ' for PTC, with R equal to 6.5, 8, and 11 Å. The resulting z values are −3, −3.3, and −4.0, respectively. Estimates of the molecular dimensions of PTC suggest a radius of 6.5 Å, whereas the correct charge of −4 is obtained only when a larger radius of 11 Å is chosen. There could be several causes for this discrepancy: (i) molecular radius and Debye–Hückel radius may not be

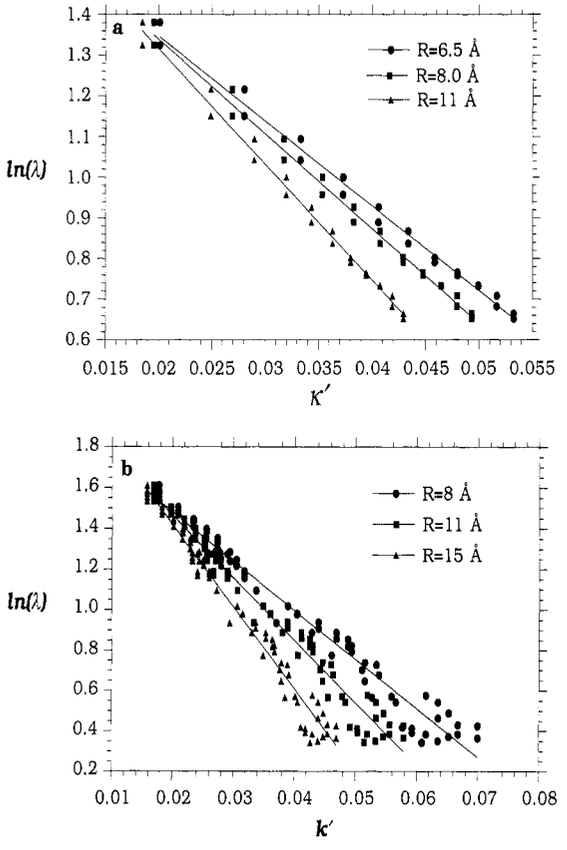

Figure 6. (a) Plot of ln λ vs κ' for PTC with R set to 6.5, 8.0, and 11.0 Å. (b) ln λ vs κ' for FA with R set to 8.0, 11.0, and 15.0 Å.

identical, especially where a substantial hydration sphere is expected; (ii) a breakdown of assumptions implicit in the Debye–Hückel analysis, e.g., a small, spherically symmetric potential and a continuous solvent; (iii) application of a steady-state theory to dynamic, molecular-scale interactions (*37*). It appears unlikely that impurities in the PTC solution (e.g., semianhydride) decreased the average charge per fluorophore in this solution since no such compounds were detected by NMR.

Despite these limitations, this analysis can provide useful information about the charge on FA. Molecular weight considerations require that FA (MW > 750) have a radius at least as large as that of PTC (MW = 424). Plots of ln λ vs κ' are shown in Figure 6b for R equal to 8, 11, and 15 Å. The slopes give z values of −3.4, −4.3, and −5.7, respectively.

Some further limits may be placed on R and z from current data on FA. Charge per molecule is based on accurate measurements of acidity equivalents per gram, and less well constrained determinations of molecular weight. For our purpose, number-average molecular weight, M_n, is more appropriate than the higher weight-averaged values; charge equivalents·M_n gives the average charge per molecule. Taking 6.1 mequiv of carboxylic acid/g (*38*) for FA, and recent M_n measurements of 711 (*39*), 829 (*33*), and 860 (*29*), gives z equal to −4.3, −5.0, or −5.2, respectively. Our data show that if PTC (R = 11 Å) is a good size analogue for FA, then z is equal to −4.3. If FA is larger than this, then a higher charge is predicted (z = −5.7 for R = 15 Å). The radius of gyration (R_g) for this material has been measured (*33*) by small-angle X-ray scattering to be 7.7 ± 0.6 Å (average of two measurements, pH = 9); other fulvic acid samples from the Suwannee River have given R_g values of 7.0 ± 0.3 and 8.8 Å (*33*). For a spherical molecule, R_g underestimates the molecular radius by ~30% (*40*).

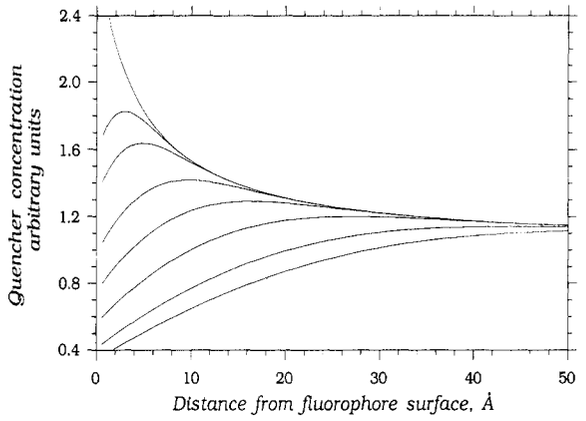

Figure 7. Schematic representation of the time evolution of the probability that a quencher with charge +1 will be within distance r of a fluorophore with charge −1. The times represented are 0, 0.05, 0.1, 0.25, 0.5, 1, 2, and 3 ns after excitation, based on the equation of Flannery (*43*) with intrinsic quenching rate equal to 5 times diffusional encounter rate.

Effect of Sample Heterogeneity. Fulvic and humic acids are heterogeneous mixtures of compounds, so the inevitable biases which this can introduce must be considered. A general question is whether the fluorescent molecules in a sample of humic material are representative of *all* molecules present; specific to quenching techniques is the question of how the results are affected by an uneven distribution of fluorescence among the molecules.

We are not aware of any technique that has successfully isolated a nonfluorescent fraction of any humic or fulvic acid, nor have any simple, free fluorophores been identified in these substances. (For example, in our work all size fractions of HA were fluorescent, but no pure fluorophores were detected.) This is a strong indication that the observed fluorescence originates from within diverse HA molecules and is not due to a few unique, separable compounds. We therefore assume, as do those who employ static quenching to measure binding coefficients (*11–14*), that the fluorescent molecules are representative of the total humic sample. Additionally, because there is no intrinsic reason why fluorescence and charge should be linked, we may assume that each fluorescent molecule contains the same charge as nonfluorescent molecules of the same size and neglect this as a significant source of error.

Neither static nor dynamic quenching depends on the number of fluorophores present; if all molecules were otherwise identical, results would not depend on what percentage of them were fluorescent. However, in a mixture of variously sized molecules, each with identical fluorescence and surface potential, the fluorescence quenching technique measures the number-averaged λ (i.e., it depends on the number of molecules present, not their mass), which tends to emphasize the smaller sized species (*41*). This bias is enhanced because large humic molecules are, as demonstrated above (Table I), less highly fluorescent than are small ones; this leads to a smaller loss of overall solution fluorescence in quenching of a large molecule than in quenching of a small one. Thus, despite its higher surface potential, the high molecular weight fraction is underrepresented in measurements of both F_0 and F, and the bias in our results should be toward the smaller and less charged molecules in each sample.

Conclusions

These experiments have demonstrated that cations are present at the surface of humic and fulvic acids in sig-

nificant excess over their concentrations in bulk solution. This effect is more pronounced at high pH where a larger fraction of acid groups are dissociated. It is also very sensitive to ionic strength, consistent with shielding of potential by electrolyte ions. Surface potential increases with molecular size in Suwannee River humic acid, as is reasonable if acid content per mass remains constant in this material. Because highly charged metal ions will be particularly susceptible to attractive potentials, this observation is of particular importance for those attempting to incorporate electrostatic effects into models of metal binding to humic substances (*6*). The surface charge calculated by a kinetic analysis of quenching data is in good agreement with predictions based on acid content and molecular weight measurements.

Acknowledgments

We thank B. Bartschat for help with theoretical aspects of humic acid electrostatics.

Appendix

The difficulties encountered in applying the steady-state kinetic model to fluorescence quenching data result from the time evolution of the probability of finding a quencher near an excited fluorophore (see, e.g., Hong and Noolandi (*42*), Flannery (*43*), Szabo (*26*), Eads et al. (*37*)) (Figure 7). At $t = 0$, corresponding to the absorption of a photon by the fluorophore, the concentration of neutral quenchers near the (negatively charged) fluorophore surface is identical to that in the bulk solution, while the concentration of cationic quenchers is higher (eq 10). At $t > 0$, the concentration of quenchers in contact with an excited fluorophore is zero because all such fluorophores have been quenched. With increasing time after excitation, the probability of finding a quencher and excited fluorophore in close proximity decreases, until, at long times, a steady state is reached. Equations 13–17 describe the steady-state situation. Thus, if the natural lifetime of the excited fluorophore is shorter than the time required to reach steady state, the measured quenching rate will be greater than that predicted by eq 13. The relevant time scale for this process can be approximated by the mean time a molecule takes to traverse a distance equal to the Debye length, $1/\kappa$, estimated from the mean diffusion time:

$$t = (\kappa^2 D)^{-1}$$

With $1/\kappa = 20$ Å ($I = 25$ mM) and $D = 10^{-5}$ cm^2 s^{-1}, this gives $t = 4$ ns. Because the time scales of fluorescence decays in solution are generally in the nanosecond range, the steady-state solution is unlikely to apply to quenching in the presence of a strong, attractive potential.

Registry No. Tempol, 2226-96-2; tempamine, 14691-88-4.

Literature Cited

(1) Zepp, R. G.; Schlotzhauer, P. F.; Sink, R. M. *Environ. Sci. Technol.* **1985**, *19*, 74–81.
(2) Faust, B. C.; Hoigné J. *Environ. Sci. Technol.* **1987**, *21*, 957–964.
(3) Waite, T. D.; Wrigley, I. C.; Szymczak, R. *Environ. Sci. Technol.* **1988**, *22*, 778–785.
(4) Dzombak, D. A.; Fish, W.; Morel, F. M. M. *Environ. Sci. Technol.* **1986**, *20*, 669–675.
(5) Fish, W.; Dzombak, D. A.; Morel, F. M. M. *Environ. Sci. Technol.* **1986**, *20*, 676–683.
(6) Bartschat, B.; Cabaniss, S. E.; Morel, F. M. M. *Environ. Sci. Technol.*, preceding article in this issue.
(7) Tipping, E.; Backes, C. A.; Hurley, M. A. *Water Res.* **1988**, *22*, 597–611.
(8) Blough, N. V. *Environ. Sci. Technol.* **1988**, *22*, 77–82.
(9) Tipping, E.; Reddy, M. M.; Hurley, M. A. *Environ. Sci. Technol.* **1990**, *24*, 1700–1705.
(10) de Wit, J. C. M.; van Riemdijk, W. H.; Nederlof, M. M.; Kinniburgh, D. G.; Koopal, L. K. *Anal. Chim. Acta* **1990**, *232*, 189–207.
(11) Saar, R. A.; Weber, J. H. *Anal. Chem.* **1980**, *52*, 2095–2100.
(12) Ryan, D. K.; Weber, J. H. *Anal. Chem.* **1982**, *54*, 986–990.
(13) Waite, T. D.; Morel, F. M. M. *Anal. Chim. Acta* **1984**, *162*, 263–274.
(14) Cabaniss, S. E.; Shuman, M. S. *Anal. Chem.* **1986**, *58*, 398–401.
(15) Green, S. A.; Simpson, D. J.; Zhou, G.; Ho, P. S.; Blough, N. V. *J. Am. Chem. Soc.* **1990**, *112*, 7337–7346.
(16) Turro, N. J. *Modern Molecular Photochemistry*, 1st ed.; Benjamin/Cummings: Menlo Park, CA, 1978; p 246.
(17) Green, J. A.; Singer, L. A.; Parks, J. H. *J. Chem. Phys.* **1973**, *58*, 2690–2695.
(18) Winiski, A. P.; Eisenberg, M.; Langner, M.; McLaughlin, S. *Biochemistry* **1988**, *27*, 386–392.
(19) Tanford, C. *Physical Chemistry of Macromolecules*, 1st ed.; John Wiley and Sons: New York, 1961; p 465.
(20) Weston, R., Jr.; Schwartz, H. A. *Chemical Kinetics*, 1st ed.; Fundamental Topics in Physical Chemistry; Prentice Hall: Englewood Cliffs, NJ, 1972; pp 151–171.
(21) Zepp, R. G.; Schlotzhauer, P. F. *Chemosphere* **1981**, *10*, 479–486.
(22) Lochmüller, C. H.; Saavedra, S. S. *Anal. Chem.* **1986**, *58*, 1978–1981.
(23) Milne, P. J.; Odem, D. S.; Zika, R. G. In *Photochemistry of Environmental Aquatic Systems*; Zika, R. G., Cooper, W. J., Eds.; ACS Symposium Series 327; American Chemical Society: Washington, DC, 1987; pp 132–140.
(24) Milne, P. J. Ph.D. Thesis, University of Miami, Miami, FL, 1989.
(25) Lappen, A. J.; Seitz, W. R. *Anal. Chim. Acta* **1982**, *134*, 31.
(26) Szabo, A. *J. Phys. Chem.* **1989**, *93*, 6929–6939.
(27) Hering, J. G. Ph.D. Thesis, MIT–WHOI Joint Program in Oceanography, 1988.
(28) Lakowicz, J. R. *Principles of Fluorescence Spectroscopy*, 1st ed.; Plenum Press: New York, 1983; p 44.
(29) Beckett, R.; Jue, Z.; Giddings, J. C. *Environ. Sci. Technol.* **1987**, *21*, 289–295.
(30) Reid, P. M.; Wilkinson, A. E.; Tipping, E.; Jones, M. N. *Geochim. Cosmochim. Acta* **1990**, *54*, 131–138.
(31) Reuter, J. H.; Perdue, E. M. *Geochim. Cosmochim. Acta* **1981**, *45*, 2017–2022.
(32) De Nobili, M.; Ghessing, E.; Sequi, P. In *Humic Substances II: In Search of Structure*; Hayes, M. H. B., MacCarthy, P., Malcolm, R. L., Swift, R. S., Eds.; John Wiley and Sons Ltd.: West Sussex, UK, 1989; pp 561–592.
(33) Aiken, G. R.; Brown, P. A.; Noyes, T. I.; Pinkney, D. J. In *Humic Substances in the Suwannee River, Georgia: Interactions, Properties, and Proposed Structures*; Averett, R. C., Leenheer, J. A., McKnight, D. M., Thorn, K. A., Eds. *Open-File Rep.—U.S. Geol. Surv.* **1989**, *No. 87-557*, 163–178.
(34) Stewart, A. J.; Wetzel, R. G. *Limnol. Oceanogr.* **1980**, *25*, 559–564.
(35) Hayase, K.; Tsubota, H. *Geochim. Cosmochim. Acta* **1985**, *49*, 159–163.
(36) Thorn, K. A. In *Humic Substances in the Suwannee River, Georgia: Interactions, Properties, and Proposed Structures*; Averett, R. C., Leenheer, J. A., McKnight, D. M., Thorn, K. A. Eds. *Open-File Rep.—U.S. Geol. Surv.* **1989**, *No. 87-557*, 251–309.
(37) Eads, D. D.; Dismer, B. G.; Fleming, G. R. *J. Chem. Phys.* **1990**, *93*, 1136–1148.
(38) Bowles, E. C.; Antweiler, R. C.; MacCarthy, P. In *Humic Substances in the Suwannee River, Georgia: Interactions, Properties, and Proposed Structures*; Averett, R. C., Leenheer, J. A., McKnight, D. M., Thorn, K. A., Eds. *Open-File Rep.—U.S. Geol. Surv.* **1989**, *No. 87-557*, 205–229.
(39) Aiken, G. R.; Malcolm, R. L. *Geochim. Cosmochim. Acta* **1987**, *51*, 2177–2184.

(40) Haschemeyer, R. H.; Haschemeyer, A. E. V. *Proteins: A Guide To Study by Physical and Chemical Methods*, 1st ed.; John Wiley and Sons: New York, 1973; p 206.
(41) Wershaw, R. L.; Aiken, G. R. In *Humic Substances in Soil, Sediment, and Water*; Aiken, G. R., McKnight, D. M., Wershaw, L. R., MacCarthy, P., Eds.; John Wiley: New York, 1985; pp 477-492.
(42) Hong, K. M.; Noolandi, J. *J. Chem. Phys.* **1978**, *68*, 5172-5176.
(43) Flannery, M. R. *Phys. Rev. A* **1982**, *25*, 3403-3406.

Received for review May 9, 1991. Revised manuscript received September 9, 1991. Accepted October 8, 1991. This work was supported by the Environmental Protection Agency under Grant CR-815293-01, by the National Science Foundation under Grant OCE-8917688, and by the Office of Naval Research under Grant N00014-89-J-1260. This is contribution No. 7734 from the Woods Hole Oceanographic Institution.

Time Persistence of Monochloramine in Human Saliva and Stomach Fluid

Tapio Kotiaho,† Joe M. Wood, Peter L. Wick, Jr., Lindy E. Dejarme, Asoka Ranasinghe, and R. Graham Cooks*

Purdue University, Department of Chemistry, West Lafayette, Indiana 47907

H. Paul Ringhand

Risk Reduction Engineering Laboratory, U.S. Environmental Protection Agency, Cincinnati, Ohio 45268

■ On-line membrane introduction mass spectrometry has been used to analyze the time persistence of monochloramine in human saliva and stomach fluid. The decay of monochloramine from a level of 0.7 ppm to levels below the detection limit (100 ppb) in saliva takes ~5 min; from a level of 1.8 ppm the decay time is ~50 min and at higher monochloramine concentrations (3.6–15 ppm) monochloramine does not react completely. This result, together with the short residence time of water in the mouth, suggests that most ingested monochloramine reaches the stomach intact. In contrast to its reaction with saliva, monochloramine decays rapidly in contact with stomach fluid; at concentrations of 0.7–15 ppm this occurs in ~30 s. This study also shows clearly the advantages of membrane introduction mass spectrometry in chloramine analysis. The ability to analyze these toxic and labile compounds directly from aqueous samples without derivatization or isolation at low detection limits is a prerequisite for establishing the biological fate of these compounds.

Introduction

Monochloramine is the second most widely used disinfectant for drinking water purification in the United States (*1*). The main advantage to using monochloramine instead of chlorine is to minimize the production of halogenated byproducts, such as the trihalomethanes. Consequently, the popularity of chloramination has increased since the maximum contaminant level (MCL) of trihalomethanes (100 μg/L) was set in 1979 (*2*); and its usage is expected to increase further if the MCL is lowered again. Therefore, faced with a possible increase in the use of chloramination for drinking water disinfection, there has been an increased interest in determining the potential health effects of inorganic chloramine(s), in identification of their byproducts, and in the potential health effects of the byproducts. In addition to the reaction of disinfectants with organic matter present in untreated water, there is also concern over the in vivo reaction of residual disinfectant present in drinking water with saliva and stomach fluid upon ingestion.

Because dialysis patients utilizing chloraminated water have been shown to develop hemolytic anemias (*3*), hematologic parameters are commonly examined in animal studies. Abdel-Rahman et al. (*4*) reported toxic effects in laboratory rats exposed to chloramine in drinking water at concentrations of 1, 10, and 100 mg/L. These toxic effects included decreased red blood cell count, glutathione content, and body weight. There was, however, a lack of a dose-dependent or time-dependent response for both hematologic parameters and glutathione levels. In a 91-day subchronic study conducted by GSRI (*5*), both rats and mice were given monochloramine in drinking water at 0, 25, 50, 100, 200, and 400 mg/L. Decreased body weights and decreased liver weights were observed for both species. Histopathological examinations indicated mild to moderate cytological alterations in the livers of male mice in the two highest dose groups. Chronic liver inflammatory changes occured in female mice at 100, 200, and 400 mg/L.

It was shown by Mink et al. (*6*) that chloroform, dichloroacetonitrile, dichloroacetic acid, and trichloroacetic acid are formed in vivo in the stomach fluid of rats administered aqueous sodium hypochlorite by gavage. It has also been shown that organic *N*-chloramines can be formed in vitro from the reaction of aqueous chlorine with amino acids present in the stomach fluid of rats (*7*). However, corresponding studies for chloramine in biological fluids have not been reported. This is probably in part due to the fact that decreased amounts of chlorinated byproducts are anticipated and there is a lack of analytical methodology that can monitor the individual inorganic chloramines.

In order to predict the feasibility of monochloramine reaching systemic circulation and hence evaluate its potential to cause toxic effects, it is important to know the time persistence of monochloramine in saliva and stomach fluid. This is the main objective of the present study. It is especially important that these measurements be made at monochloramine levels (1–3 ppm) typically present in drinking water (*8*). This latter requirement has been addressed recently by Scully and White (*9*) in an article which reviewed the current knowledge of the chemistry of monochloramine with organic and inorganic constituents in saliva and stomach fluid. Recent developments with respect to membrane introduction mass spectrometry (MIMS) have made it possible to accomplish this task, since it has been shown that MIMS can be used to measure monochloramine directly from aqueous solutions at sub-part-per-million levels (*10*).

† On leave from Technical Research Center of Finland, Chemical Laboratory, Biologinkuja 7, 02150 Espoo, Finland.

 0013-936X/92/0926-0302$03.00/0